Phase transition in the three dimensional Heisenberg spin glass: Finite-size scaling analysis

L. A. Fernandez,[1,2] V. Martin-Mayor,[1,2] S. Perez-Gaviro,[2,3] A. Tarancon,[2,4] and A. P. Young[5]
[1]*Departamento de Física Teórica I, Universidad Complutense, 28040 Madrid, Spain*
[2]*Instituto de Biocomputación y Física de Sistemas Complejos (BIFI), 50009 Zaragoza, Spain*
[3]*Dipartimento di Fisica, SMC of INFM-CNR and INFN, Università di Roma La Sapienza, 00185 Roma, Italy*
[4]*Departamento de Física Teórica, Universidad de Zaragoza, 50009 Zaragoza, Spain*
[5]*Department of Physics, University of California, Santa Cruz, California 95064, USA*
(Received 4 May 2009; published 22 July 2009)

We have investigated the phase transition in the Heisenberg spin glass using massive numerical simulations to study very large sizes, 48^3. A finite-size scaling analysis indicates that the data are compatible with the most economical scenario: a common transition temperature for spins and chiralities.

DOI: 10.1103/PhysRevB.80.024422 PACS number(s): 75.10.Nr, 05.50.+q, 75.40.Mg, 75.50.Lk

I. INTRODUCTION

As a result of extensive and careful numerical studies,[1–3] there is now compelling evidence for a finite-temperature phase transition in the Ising spin glass in three dimensions. However, the situation for the Heisenberg spin glass, in which the spins are classical 3-component vectors, is still controversial. The Heisenberg spin glass is a suitable first model to describe experimental systems with weak anisotropy, such as dilute Mn atoms in Cu which is a well-studied spin-glass system, see, e.g., Ref. 4. Kawamura[5,6] proposed that the spin-glass transition only occurs at $T_{\rm SG}=0$ and that a *chiral*-glass transition occurs at a finite temperature $T_{\rm CG}$. Chiralities are Ising-type variables which describe the handedness of the noncollinear spin structure. This scenario requires that spins and chiralities decouple at long length scales. However, simulations[7–9] subsequently found evidence for a finite $T_{\rm SG}$, though corrections to the leading finite-size scaling behavior seem larger than in the Ising case.[3] Recently, Viet and Kawamura,[10,11] who did a similar analysis to that of Refs. 8 and 9 and used the same range of sizes ($L\leq 32$, where L is the linear size of the system), concluded that $T_{\rm SG}$ is indeed finite but is less than $T_{\rm CG}$ which still implies spin-chirality decoupling.

In view of this controversy over the nature of the transition in the three dimensional Heisenberg spin glass, which is of great importance for the understanding of spin glasses, we have undertaken a massive set of simulations to study even larger sizes,[12] $N=L^3$ where $L\leq 48$. Our conclusion is that the data *are* consistent with a common transition temperature for spins and chiralities, though, of course, numerics can never prove that they are *exactly* equal.

The paper is organized as follows. In Sec. II we define the model and the observables. Finite-size scaling, which is central in our analysis, is recalled in Sec. III. Simulation details are in Sec. IV while our equilibration tests are addressed in Sec. V. We find that a uniform allocation of computational resources is inefficient (equilibration is much harder to achieve for some particular samples). The numerical results are in Sec. VI while our conclusions are presented in Sec. VII.

II. MODEL AND OBSERVABLES

We use the standard Edwards-Anderson spin-glass model on a cubic lattice

$$\mathcal{H}=-\sum_{\langle i,j\rangle} J_{ij}\mathbf{S}_i\cdot\mathbf{S}_j, \tag{1}$$

where the $\mathbf{S}_i$ are 3-component classical vectors of unit length at the sites of a simple cubic lattice and the J_{ij} are nearest-neighbor interactions with a Gaussian distribution with zero mean and standard deviation equal to unity. Periodic boundary conditions are applied.

The spin-glass order parameter is $q_i^{\mu\nu}=S_i^{\mu(1)}S_i^{\nu(2)}$, where "(1)" and "(2)" are two identical copies of the system (same interactions) and ν and μ are spin components. Its Fourier transform at wave vector $\boldsymbol{k}$ is denoted by $\hat{q}^{\mu\nu}(\boldsymbol{k})$.

For the Heisenberg spin glass, Kawamura[5] defines the *chirality* from spins on a line as $\kappa_i^{\mu}=\mathbf{S}_{i+\hat{\mu}}\cdot(\mathbf{S}_i\times\mathbf{S}_{i-\hat{\mu}})$, where μ refers to a direction on the lattice. The related chiral spin-glass order parameter is $q_{{\rm CG},i}^{\mu}=\kappa_i^{\mu(1)}\kappa_i^{\mu(2)}$, its Fourier transform being $\hat{q}_{\rm CG}^{\mu}(\boldsymbol{k})$.

The wave-vector-dependent susceptibilities are computed from the two order parameters

$$\chi_{\rm SG}(\boldsymbol{k})=N\sum_{\mu,\nu}[\langle|\hat{q}^{\mu\nu}(\boldsymbol{k})|^2\rangle]_{\rm av}, \tag{2}$$

$$\chi_{\rm CG}^{\mu}(\boldsymbol{k})=N[\langle|\hat{q}_{\rm CG}^{\mu}(\boldsymbol{k})|^2\rangle]_{\rm av}, \tag{3}$$

where $\langle\cdots\rangle$ denotes a thermal average and $[\cdots]_{\rm av}$ denotes an average over disorder.

The susceptibilities yield the second-moment finite-lattice estimator of the correlation length[1,13–15]

$$\xi_L=\frac{1}{2\sin(\pi/L)}\sqrt{\frac{\chi(0)}{\chi(\boldsymbol{k}_{\rm min})}-1}, \tag{4}$$

with $\boldsymbol{k}_{\rm min}=(2\pi/L,0,0)$. The spin and chiral[16] correlation lengths are denoted by $\xi_{{\rm SG},L}$ and $\xi_{{\rm CG},L}$, respectively.

We also consider the spin and chiral Binder ratios defined by

$$g_{\rm SG}=\frac{11}{2}-\frac{9[\langle q^4\rangle]_{\rm av}}{2[\langle q^2\rangle]_{\rm av}^2},\quad g_{\rm CG}=\frac{5}{2}-\frac{3[\langle q_{\rm CG}^4\rangle]_{\rm av}}{2[\langle q_{\rm CG}^2\rangle]_{\rm av}^2}, \tag{5}$$

where $q^2=\Sigma_{\mu\nu}[\hat{q}^{\mu\nu}(\boldsymbol{k}=0)]^2$ and $q_{\rm CG}^2=\Sigma_{\mu}[\hat{q}_{\rm CG}^{\mu}(\boldsymbol{k}=0)]^2$.

III. FINITE-SIZE SCALING

Finite-size scaling is a most useful data-analysis method that exploits finite-size effects where they are largest (at criticality) to gather information on the *infinite* system, see, e.g., Ref. 15. Finite-size scaling takes the form of an asymptotic expansion on the system size, L. To leading order, for a quantity O diverging in the thermodynamic limit as $O \propto |T - T_c|^{x_O}$, it takes the form

$$O(L,T) = L^{x_O/\nu} f[L^{1/\nu}(T - T_c)], \tag{6}$$

where f is an analytic function of its argument. In particular, since $\xi_{SG,L}/L$ is dimensionless it has the finite-size scaling form[1,7,17,18]

$$\frac{\xi_{SG,L}}{L} = \tilde{X}[L^{1/\nu}(T - T_{SG})], \tag{7}$$

where ν is the correlation length exponent. There are similar expressions for $\xi_{CG,L}/L$ and also for the Binder ratios in Eq. (5) since these too are dimensionless.

We shall see that corrections to scaling are quite large, even for the large sizes that we study, and so we need to consider *corrections* to the asymptotic scaling form in Eq. (7). To investigate this we determine the intersection temperatures $T^{\star}_{SG}(L,sL)$, where the data for $\xi_{SG,L}/L$ agree for sizes L and sL, i.e.,

$$\frac{\xi_{SG,L}}{L} = \frac{\xi_{SG,sL}}{sL}, \tag{8}$$

with an analogous expression for the chiral data.

Although Eq. (7) predicts that all the $T^{\star}_{SG}(L,sL)$ are equal to the spin-glass transition temperature T_{SG}, when one includes the leading corrections to scaling, the $T^{\star}_{SG}(L,sL)$ are given by[3,17,18]

$$T^{\star}_{SG}(L,sL) - T_{SG} = A^{(s)}_{SG} L^{-\omega-1/\nu}. \tag{9}$$

Here, ω is the exponent for the leading correction to scaling while the amplitude is

$$A^{(s)}_{SG} = A_{SG} \frac{1 - s^{-\omega}}{s^{1/\nu} - 1}, \tag{10}$$

with A_{SG} a (nonuniversal) constant. In practice, we do not have enough information to determine the s dependence in Eq. (9), so we take the $A^{(s)}_{SG}$ to be separate constants for each value of s that we use ($s=2$ and 3/2).

In fact we may combine Eqs. (6) and (8) to obtain a modern form of Nightingale's phenomenological renormalization,[19] the so-called quotient method,[18]

$$\frac{O(sL, T^{\star}_{SG}(L,sL))}{O(L, T^{\star}_{SG}(L,sL))} = s^{x_O/\nu_{SG}}[1 + \tilde{A}_{O,s} L^{-\omega} + \ldots], \tag{11}$$

where the dots stand for higher-order scaling corrections. Were T_{CG} and T_{SG} different, a similar expression would hold for quantities diverging at T_{CG}. In particular, one may use Eq. (11) with temperature derivatives (to obtain $1+1/\nu$) or with the susceptibilities at zero wave number (to obtain $2 - \eta$, where η is the anomalous dimension).

TABLE I. Parameters of the simulations. N_T is the number of temperatures. For the larger sizes, the number of sweeps varied from sample to sample. We show values for $N^{\min}_{\text{sweep}}$ and $N^{\max}_{\text{sweep}}$, the minimum and maximum number of overrelaxation sweeps.

L	$N^{\min}_{\text{sweep}}$	$N^{\max}_{\text{sweep}}$	N_T	N_{samp}
8	5.0×10^5	5.0×10^5	5	984
12	7.5×10^5	7.5×10^5	9	984
16	1.0×10^6	1.0×10^6	15	984
24	1.5×10^6	1.2×10^7	27	984
32	4.0×10^6	1.2×10^8	43	984
48	6.0×10^7	6.0×10^8	79	164

IV. SIMULATION DETAILS

Simulations are run in parallel on N_T processors at N_T different temperatures using the parallel tempering[20] (PT) method to speed up equilibration at low T, see Table I for the parameters.

As discussed in other work,[8–10] three types of moves are performed: (i) "overrelaxation" (OR) sweeps (which do not change the energy), (ii) "heat-bath" (HB) sweeps (which do change the energy), and (iii) PT sweeps in which the spin configurations at neighboring temperatures are swapped with a probability which satisfies the detailed balance condition. It is important to include OR sweeps because not only is the code for them much simpler (and hence faster) than that for the HB sweeps, but also because OR moves are very efficient[8,9,21] in equilibrating the system, so *fewer* sweeps are required than in a simulation with only HB and PT moves. Nonetheless, a fraction of the moves must be HB in order to change the energy. Because of the PT moves, the temperature of a set of spins (a "copy") is not fixed but does a random walk between the minimum and maximum temperature in the set. In this way, each copy of spins can visit different "valleys" in configuration space with the correct statistical weight, even at low temperature.

The N_T temperatures were arranged in a geometric progression between $T_{\min}=0.12$ and $T_{\max}=0.19$. We do 1 HB sweep followed by $5L/4$ OR sweeps and then 100 PT sweeps. We found a net CPU gain by doing a number of OR sweeps between HB sweeps which is somewhat greater than L, perhaps because this transfers a fluctuation right across the system. We do a large number (100) of PT sweeps one after another because the PT sweeps are very inexpensive in CPU time.

V. EQUILIBRATION

We do several tests to ensure equilibration. First, we require that data satisfy the relation[9,22]

$$\Delta \equiv \left[\frac{q_s - q_1}{T} + \frac{2}{z} U \right]_{\text{av}} = 0, \tag{12}$$

which is valid for a Gaussian bond distribution. Here

$$U = -\sum_{\langle i,j \rangle} J_{ij} \langle \mathbf{S}_i \cdot \mathbf{S}_j \rangle, \tag{13}$$

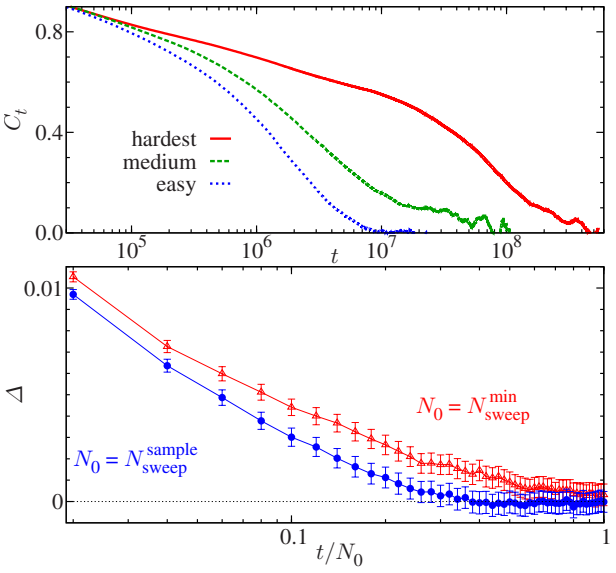

FIG. 1. (Color online) Top: parallel tempering autocorrelation function (Ref. 23), as computed for three representative $L=48$ samples. Here easy means that after $N^{\rm min}_{\rm sweep}$ MC steps, see Table I, the equilibration criterion was met (42% of samples), while *medium* samples (34%) required up to $2N^{\rm min}_{\rm sweep}$ MC steps. Bottom: the quantity Δ in Eq. (12) as a function of MC time, both in units of $N^{\rm min}_{\rm sweep}$ (red triangles) and in units of the maximum number of sweeps for each sample (blue circles). For the latter, note that the data are computed at different times for different samples.

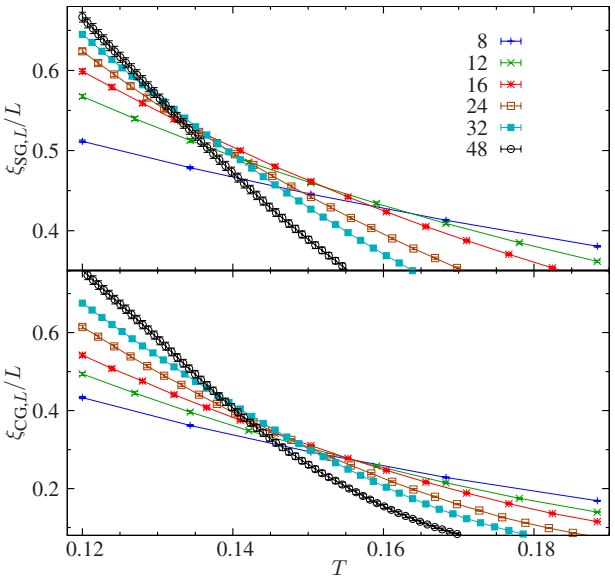

FIG. 2. (Color online) Data for the spin-glass and chiral-glass correlation lengths divided by system size. For $L\to\infty$ the data should intersect at the transition temperature. Here, the data do not show a common intersection temperature indicating that there are strong corrections to scaling for the range of sizes studied.

$$q_{\rm l} = (1/N_{\rm b})\sum_{\langle i,j\rangle} \langle \mathbf{S}_i \cdot \mathbf{S}_j\rangle^2, \tag{14}$$

$$q_{\rm s} = (1/N_{\rm b})\sum_{\langle i,j\rangle} \langle (\mathbf{S}_i \cdot \mathbf{S}_j)^2\rangle, \tag{15}$$

in which U is the thermally averaged energy per spin, $q_{\rm l}$ is called the "link overlap," $N_{\rm b}=(z/2)N$ is the number of nearest-neighbor bonds, and z (=6 here) is the lattice coordination number. Both U and $q_{\rm s}$, being a single thermal average, come close to equilibrium relatively quickly as the number of Monte Carlo (MC) sweeps increases. However, $q_{\rm l}$ involves a double thermal average which is determined from two separate copies initialized with random spin configurations and, hence, is initially very small. As the simulation proceeds, $q_{\rm l}$ increases toward its equilibrium value, so Δ in Eq. (12) will initially be positive but will become zero (and stay zero) when equilibrium is reached. Data are shown in Fig. 1 for $L=48$ (the largest size) at $T=0.12$ (the lowest temperature).

Equation (12) also provides a *control variate*[24] to reduce statistical errors in $\xi_{{\rm SG},L}$ and $\xi_{{\rm CG},L}$. The key is in the strong statistical correlations between the Monte Carlo estimator for Δ and those for the susceptibilities. Since we happen to know that $\Delta=0$, reduced-variance estimators for the susceptibilities are obtained straightforwardly (see Ref. 24 for details). In practice, this method halves the errors for $\xi_{\rm CG,SG}$ at $T=0.12$ (however, for $T\gtrsim 0.14$ the gain is less than 10%).

Some samples are harder to equilibrate than others so, ideally, we should spend more MC sweeps on the "hard" ones than on "easy" ones. The key to classifying samples in a PT simulation is to consider the dynamics of the temperature random walk. In hard samples, the T random walk is slower (a copy trapped in a deep valley needs a longer time to wander to a T high enough to escape). We use correlation functions and autocorrelation times to formalize this idea, see Fig. 1 and the comments in Ref. 23.

For each sample, we impose a minimum number of sweeps, Table I, and then keep simulating until the total number of MC iterations exceed 9 autocorrelation times. For $L=48$, the average number of MC iterations per sample was 1.8 times the minimum. Figure 1 shows that the data equilibrate more convincingly by running the hard samples for longer than the easy samples.

VI. RESULTS

We now present our results. Figure 2 shows data for the spin-glass and chiral-glass correlation lengths divided by L. The resulting intersection temperatures obtained from a jackknife analysis are shown in Table II.

Since Eq. (9) holds only asymptotically, for large L it is necessary to decide on the smallest size $L_{\rm min}$ to be included in the analysis. We consider first the five pairs of sizes with $L_{\rm min}=12$, see Table II. Fitting spin and chiral data separately, there are four parameters for each: $T_{\rm CG,SG}$, the exponent $\omega + 1/\nu$, and amplitudes $A^{(2)}_{\rm CG,SG}$ and $A^{(3/2)}_{\rm CG,SG}$ for the $s=2$ and $s=3/2$ size ratios. We determine the best fit parameters and estimate the quality of the fit from[25] the value of χ^2. Fitting the spin data to Eq. (9) gives $T_{\rm SG}=0.129^{+0.003}_{-0.016}$, which is compatible with Viet and Kawamura's result of 0.120(6). However, in the chiral sector χ^2 as a function of $T_{\rm CG}$ does not have a local minimum with $T_{\rm CG}>0$, so subleading scaling

TABLE II. Table of intersection temperatures $T^\star(L,sL)$ for the spin-glass and chiral-glass correlation-length data presented in Fig. 2. Also shown are estimates for the exponents ν and $2-\eta$ for the case of $s=2$, using the quotient method (Refs. 15 and 18), see Eq. (11). The operators used are $\partial_T \xi_{SG,L}$, $\partial_T \xi_{CG,L}$ χ_{SG}, and χ_{CG} which have scaling exponents $1+1/\nu_{SG}$, $1+1/\nu_{CG}$, $2-\eta_{SG}$, and $2-\eta_{CG}$, respectively. Spin (chiral) exponents are computed from data at $T^\star_{SG}(L,sL)$ ($T^\star_{CG}(L,sL)$).

L	sL	$T^\star_{SG}$	$T^\star_{CG}$	ν_{SG}	ν_{CG}	$2-\eta_{SG}$	$2-\eta_{CG}$
8	16	0.158(1)	0.156(1)	1.01(2)	1.34(5)	1.99(1)	0.72(2)
12	24	0.142(2)	0.150(1)	1.35(5)	1.51(6)	2.08(1)	0.96(3)
16	32	0.136(1)	0.147(1)	1.50(7)	1.46(6)	2.14(1)	1.11(3)
24	48	0.133(2)	0.142(1)	1.49(13)	1.30(8)	2.19(2)	1.44(4)
8	12	0.164(2)	0.157(2)				
16	24	0.135(2)	0.147(2)				
32	48	0.130(3)	0.138(2)				

corrections are sizable for chiralities and $L_{min}=12$.

Hence we have also performed an analysis with a larger value, $L_{min}=16$. Unfortunately, we only have data for four pairs of sizes and still four parameters to be fitted if we fit the spin and chiral data separately. Since the number of points is equal to the number of parameters we do not gain useful information. However, if we assume a *common transition temperature* and do a joint fit, we have eight data points and six parameters (one transition temperature, one exponent, and four amplitudes). The resulting fit gives $T_c(=T_{SG}=T_{CG})=0.120^{+0.010}_{-0.100}$ with a χ^2 per degree of freedom of 0.029, so the fit is good. The error bar on T_c is very large on the low-T side but if we assume that the exponent $1/\nu+\omega$ in Eq. (9) is greater than 0.5, plausible given the values for ν in Table II, we find $T_c=0.120^{+0.010}_{-0.004}$, which is much more tightly constrained.

In Fig. 3 we show data for the spin-glass and chiral-glass Binder ratios defined in Eq. (5). Our definition of g_{CG} differs from that of Kawamura and Viet[10] and our results have an even more pronounced negative dip. Interestingly, we find that the results for g_{SG} *also* become negative at the largest sizes. Hence, the apparent vanishing of g_{SG} near T_{CG}, a strong argument for spin-chirality decoupling,[6] is an artifact caused by the lattice sizes being too small and the temperatures too high. Our interpretation of the Binder parameter data is that there is negative dip in both channels and the minimum of this dip approaches the transition temperature as L grows. The chiral dip approaches T_{CG} from high temperatures, while the spin dip approaches T_{SG} from low temperatures, where plausibly $T_{SG}=T_{CG}$. However, much larger sizes would be needed to confirm this hypothesis.

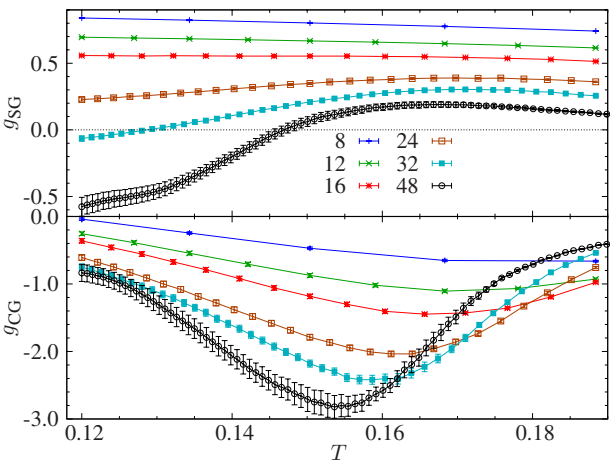

FIG. 3. (Color online) Data for the spin-glass and chiral-glass Binder ratios defined in Eq. (5) of the text.

By studying sizes $L\leq 32$, Viet and Kawamura[10,11] find $T_{SG}=0.120(6)$ and $T_{CG}=0.145(4)$. Since the difference is about 3.5 times the errors, they argue that $T_{CG}>T_{SG}$. However, their value for T_{CG} is actually higher than our intersection temperatures for $L=48$ shown in Table II and, hence, seems to us to be too high. Also they estimate the transition temperatures from $T^\star(L,sL)-T_{CG}=\text{const.}/L_{av}$, where L_{av} is the average of L and sL, rather than Eq. (9). In other words they replace the exponent $\omega+1/\nu$ by 1 and the s dependence in Eq. (9) by $2/(1+s)$. At the very least, we argue that these replacements lead to an underestimate of the error bars. Hence, we do not feel that the results of Viet and Kawamura contradict our conclusion that the data are consistent with the spin- and chiral-glass transition temperatures being equal.

VII. CONCLUSIONS

In summary, our low-temperature simulations for the Heisenberg spin glass used very large system sizes. To achieve thermalization, we needed not only a huge amount of CPU time (7×10^6 hours) but a careful sample-by-sample thermalization check that allowed us to concentrate efforts on the hard samples. The results for the spin-glass sector can be accounted for using only leading-order scaling corrections but subleading corrections are sizable for the chiral-glass sector. This is the reason for the overestimate of T_{CG} in previous work.[10,11] Data for $L\geq 16$ support the most economic scenario, $T_{SG}=T_{CG}$. We also see that the spin Binder parameter is *not* trivial at T_{CG}.

ACKNOWLEDGMENTS

The CPU time used was 1.3×10^6 hours at CINECA (through the EU DEISA initiative), 4.7×10^6 hours at the Mare Nostrum, 10^6 hours at Caesaraugusta, and 10^5 hours at the Hierarchical Systems Research Foundation. We were

partly supported by MICINN (Spain, research Contract No. FIS2006-08533-C03). The authors thankfully acknowledge the computer resources, technical expertise, and assistance provided by the staff at the *Red Española de Supercomputación–Barcelona Supercomputing Center* and at CINECA.

[1] H. G. Ballesteros, A. Cruz, L. A. Fernandez, V. Martin-Mayor, J. Pech, J. J. Ruiz-Lorenzo, A. Tarancon, P. Tellez, C. L. Ullod, and C. Ungil, Phys. Rev. B **62**, 14237 (2000).

[2] H. G. Katzgraber, M. Körner, and A. P. Young, Phys. Rev. B **73**, 224432 (2006).

[3] M. Hasenbusch, A. Pelissetto, and E. Vicari, Phys. Rev. B **78**, 214205 (2008).

[4] R. Omari, J. J. Prejean, and J. Souletie, J. Phys. (Paris) **44**, 1069 (1983).

[5] H. Kawamura, Phys. Rev. Lett. **80**, 5421 (1998).

[6] K. Hukushima and H. Kawamura, Phys. Rev. B **72**, 144416 (2005).

[7] L. W. Lee and A. P. Young, Phys. Rev. Lett. **90**, 227203 (2003).

[8] I. Campos, M. Cotallo-Aban, V. Martin-Mayor, S. Perez-Gaviro, and A. Tarancon, Phys. Rev. Lett. **97**, 217204 (2006).

[9] L. W. Lee and A. P. Young, Phys. Rev. B **76**, 024405 (2007).

[10] D. X. Viet and H. Kawamura, Phys. Rev. Lett. **102**, 027202 (2009).

[11] D. X. Viet and H. Kawamura, arXiv:0904.3699 (unpublished).

[12] To our knowledge, a 48^3 lattice is the largest spin glass that has been thermalized near a finite-temperature phase transition. It is curious that larger sizes can be studied for the Heisenberg model than for the Ising cases [for which the 28^3 samples studied by Hasenbusch *et al.* (Ref. 3) seems to be the record], even though the updating code is more complicated. Evidently, the barriers between valleys are lower in the Heisenberg model.

[13] B. Cooper, B. Freedman, and D. Preston, Nucl. Phys. B **210**, 210 (1982).

[14] M. Palassini and S. Caracciolo, Phys. Rev. Lett. **82**, 5128 (1999).

[15] D. Amit and V. Matin-Mayor, *Field Theory, the Renormalization Group and Critical Phenomena* (World Scientific, Singapore, 2005).

[16] For the CG, one considers a transverse or parallel $\xi_{CG,L}$, depending on whether $\hat{\mu}\cdot\boldsymbol{k}_{\min}=0$ or not (Refs. 7 and 8). We report only the parallel $\xi_{\mathrm{CG},L}$ as the two coincide within errors.

[17] K. Binder, Z. Phys. B: Condens. Matter **43**, 119 (1981).

[18] H. G. Ballesteros, L. A. Fernández, V. Martín-Mayor, and A. Muñoz Sudupe, Phys. Lett. B **387**, 125 (1996).

[19] M. P. Nightingale, Physica A **83**, 561 (1975).

[20] K. Hukushima and K. Nemoto, J. Phys. Soc. Jpn. **65**, 1604 (1996).

[21] J. H. Pixley and A. P. Young, Phys. Rev. B **78**, 014419 (2008).

[22] H. G. Katzgraber, M. Palassini, and A. P. Young, Phys. Rev. B **63**, 184422 (2001).

[23] Given the set of temperatures $\{T_i\}$, let $f(T)$ be a cubic polynomial in T^{-1} (unique up to an irrelevant multiplicative constant) with $\Sigma_i f(T_i)=0$ and $f'(T_{\max})=0$, and changing sign at $0.14\approx T_c$. Let f_t be $f(T)$ for the T occupied by one copy of the system at time t. We first coarse grain f_t by averaging over 100 consecutive MC sweeps and then compute its autocorrelation function and integrated autocorrelation time (Refs. 15 and 26).

[24] L. A. Fernandez and V. Martin-Mayor, Phys. Rev. E **79**, 051109 (2009).

[25] The $T^*_{\mathrm{SG,CG}}(L,sL)$ are statistically correlated, so one should use the full covariance matrix to compute χ^2. However, we find that considering only diagonal covariances does not significantly change the results. We give results obtained with diagonal covariances since these can be reproduced from the data in Table II.

[26] A. Sokal, in *Functional Integration: Basics and Applications*, edited by C. DeWitt-Morette, P. Cartier, and A. Folacci (Plenum, New York, 1997).